Temperature and Pressure Dependent Rate Coefficients for the Reaction of Hg with Cl and the Reaction of Cl with Cl: A Pulsed Laser Photolysis−Pulsed Laser Induced Fluorescence Study

Deanna L. Donohoue, Dieter Bauer, and Anthony J. Hynes*

Division of Marine and Atmospheric Chemistry, Rosenstiel School of Marine and Atmospheric Science, University of Miami, 4600 Rickenbacker Causeway, Miami, Florida 33149

Received: March 15, 2005; In Final Form: July 5, 2005

A pulsed laser photolysis−pulsed laser induced fluorescence technique has been employed to study the recombination of mercury and chlorine atoms, Hg + Cl + M → HgCl + M (1), and the self-reaction of chlorine atoms, Cl + Cl + M → Cl_2 + M (2). Rate coefficients were determined as a function of pressure (200−600 Torr) and temperature (243−293 K) in N_2 buffer gas and as a function of pressure (200−600 Torr) in He buffer gas at room temperature. For reaction (1) kinetic measurements were obtained under conditions in which either mercury or chlorine atoms were the reactant in excess concentration while simultaneously monitoring the concentration of both reactants. An Arrhenius expression of $(2.2 \pm 0.5) \times 10^{-32}$ exp{$(680 \pm 400)(^1/_T - {}^1/_{298})$} cm^6 molecule^{-2} s^{-1} was determined for the third-order recombination rate coefficient in nitrogen buffer gas. The effective second-order rate coefficient for reaction 1 under atmospheric conditions is much smaller than prior determinations using relative rate techniques. For reaction (2) we obtain an Arrhenius expression of $(8.4 \pm 2.3) \times 10^{-33}$ exp{$(850 \pm 470)(^1/_T - {}^1/_{298})$} cm^6 molecule^{-2} s^{-1} for the third-order recombination rate coefficient in nitrogen buffer gas. The rate coefficients are reported with a 2σ error of precision only; however, due to the uncertainty in the determination of absolute chlorine atom concentrations we conservatively estimate an uncertainty of ±50% in the rate coefficients. For both reactions the observed pressure, temperature, and buffer gas dependencies are consistent with the expected behavior for three-body recombination.

Introduction

Mercury (Hg) is one of the most toxic elements in nature. It has been linked to the decline of the Florida Panther,[1] reproductive anomalies in avian species, such as the loon (*Gavia immer*)[2] and the warbler (*Prothonotaria citrea*),[1] and neurological damage to humans.[3] Exposure to mercury is primarily through the ingestion of dimethylmercury from food sources. Therefore, to determine the impacts of this toxin, most studies have focused on the terrestrial and aquatic cycling of mercury. However, over the past decade there has been a recognition that the atmospheric cycling of mercury directly influences both terrestrial and aquatic systems, and thus an understanding of the atmospheric cycle is essential to understanding the overall biogeochemical cycling of mercury.

Atmospheric mercury exists in three major forms, gaseous elemental mercury, reactive gaseous mercury, and particulate mercury. Gaseous elemental mercury is thought to be the major constituent typically accounting for over 90% of gas-phase mercury.[4] Until recently it was believed that this species was relatively unreactive in the gas phase, resulting in an atmospheric lifetime of 6 months to a year.[4] Recent measurements in the Arctic,[5,6] Antarctic,[7,8] Greenland,[9] and Norway[10] indicate that a rapid gas-phase oxidation process does occur.

Although these recent measurements indicate that there is an atmospheric transformation occurring, the exact mechanism has yet to be identified. To understand the cycling of mercury in terrestrial and aquatic systems and the potential affects of mercury on human and ecological health, it is essential to identify this transformation. Mercury events correlate well with tropospheric ozone depletion events, which are known to be triggered by the photolysis of labile halogen species, released from snowpack at polar sunrise.[11] It has been suggested that the mercury transformation mechanism is driven by halogen chemistry. The implications of this for atmospheric mercury chemistry on a global scale are unclear because the precise mechanism of this transformation is not known and very few data are available for rate coefficients for reactions of elemental mercury with halogen radicals.

In this work we report direct measurements of the rate coefficient for the reaction of elemental mercury with chlorine atoms, as a function of temperature and pressure in nitrogen and helium buffer gases.

$$\mathrm{Hg + Cl + M \rightarrow HgCl + M} \qquad (1)$$

Kinetic measurements were performed with each of the reactants in excess concentration, with temporal profiles of both reactants being monitored by LIF. Measurements made under conditions in which Cl atoms were the reactant in excess concentration required an accurate concentration calibration and must account for the chlorine atom recombination. Consequently, we also measured the rate coefficient for the recombination of chlorine atoms, under similar experimental conditions.

$$\mathrm{Cl + Cl + M \rightarrow Cl_2 + M} \qquad (2)$$

There have been three prior experimental determinations[12−14] of the rate coefficient for reaction 1 and one theoretical study.[15]

* To whom correspondence should be addressed.

10.1021/jp051354l CCC: $30.25
Published on Web 08/10/2005

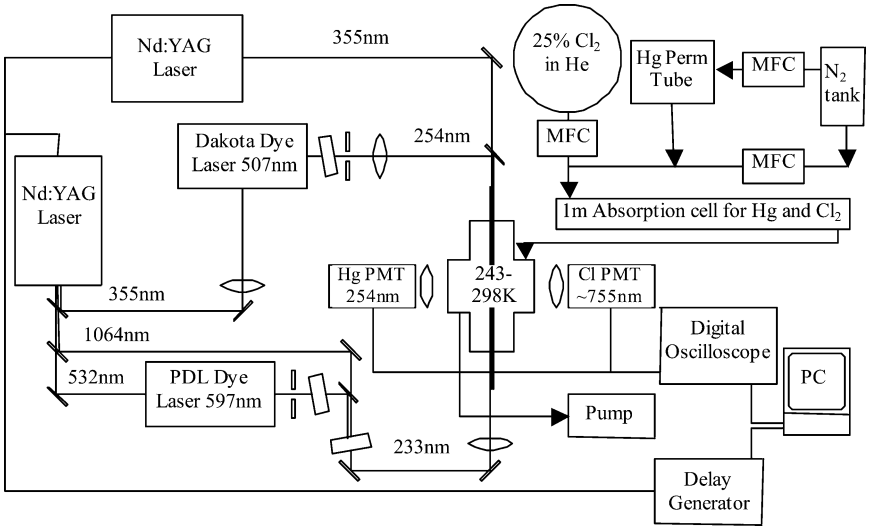

Figure 1. Experimental setup for the PLP−PLIF system to detect Hg by one photon LIF and Cl atom by two photon LIF, including optical and flow system configurations.

We report rate coefficients that are significantly slower than those obtained in prior studies.

Experimental Section

The reaction between gaseous elemental mercury and chlorine atoms was studied by pulsed laser photolysis−pulsed laser induced fluorescence (PLP−PLIF) as a function of pressure and temperature in nitrogen, helium, and air buffer gas. Experiments were conducted at three temperatures 293, 263, and 243 K, and three pressures, 200, 400, and 600 Torr.

Chlorine atoms were produced by pulsed laser photolysis of molecular chlorine. The temporal profiles of both chlorine atoms and mercury atoms were monitored by two- and one-photon laser induced fluorescence (LIF), respectively. The experimental configuration is detailed in Figure 1. The experiments were conducted in a temperature controlled Pyrex reaction vessel. Four mutually perpendicular sidearms with quartz windows were attached to the center of the vessel. The photolysis and the probe lasers were overlapped using dichroic mirrors and then propagated through two of the cell's sidearms, perpendicular to the gas flow. The temperature of the reaction vessel was controlled by a circulating methanol bath while the windows were constantly flushed with dry air to prevent condensation. A thermocouple was inserted into the reaction zone through a vacuum seal, allowing measurement of the gas temperature under the precise pressure and flow conditions of the experiment.

Experiments were carried out under "slow-flow" conditions. The gas velocity was maintained at approximately 13 cm s^{-1}, to completely replace the gas mixture in the reaction zone between the laser pulses. All flows were monitored using calibrated mass flow controllers. The pressure was monitored with a capacitance manometer.

Chlorine atoms were produced by photolysis of molecular chlorine using the 355 nm, third harmonic of a Nd:YAG laser.

$$Cl_2 + h\nu \rightarrow Cl + Cl \qquad (3)$$

An output power of approximately 350 mJ per pulse resulted in chlorine concentrations ranging from 2.5×10^{15} to 13×10^{15} molecules cm^{-3}. The photolysis of molecular chlorine at 355 nm from the ground state, $^1\Sigma_g^+$, to the repulsive exited state, $^1\Pi_{1u}$, generates chlorine atoms almost exclusively in the $^2P^0_{3/2}$ ground state.[16] This results in a quantum yield for the photolysis of molecular chlorine[17] of 2.

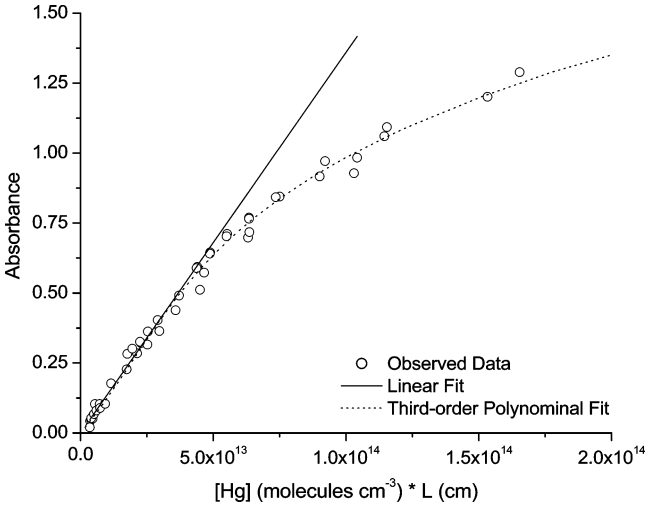

Figure 2. Absorbance verses mercury concentration ([Hg]) × path length (*L*), illustrating the deviation from the Beer−Lambert law.

The buffer gas flowed over a mercury permeation tube with a permeation rate between 120 and 7000 ng min^{-1} depending on temperature. This produced stable mercury concentrations, which ranged from 1×10^{12} to 60×10^{12} molecules cm^{-3} under our flow conditions.

Elemental mercury and molecular chlorine concentrations were monitored in situ by UV photometry using the 253.7 and 365 nm lines from a mercury lamp, respectively. The reaction mixture was flowed through a 1 cm or 1 m absorption cell depending on mercury concentration. After passage through the absorption cell the lamp output was split with a dichroic beam splitter and detected by two interference filter/photomultiplier (PMT) combinations and each absorbance was recorded.

Because the line width of the mercury absorption line is narrower than the broadened output of the mercury lamp, the effective cross-section depends on the line width of the lamp, requiring a determination of the effective absorption cross-section. This was determined by monitoring absorbance as a function of path length and Hg concentration. Mercury concentrations were generated using a calibrated permeation tube at 100 °C and were confirmed by analysis with a Tekran 2537A mercury analyzer. Figure 2 shows a plot of absorbance verses mercury concentration ([Hg]) × path length (L) illustrating the deviation from the Beer−Lambert law. For absorbances less

than 0.7 the Beer−Lambert law held and the effective cross-section was 1.36×10^{-14} cm^2. For absorbances greater than 0.7 there was a significant deviation from the Beer−Lambert law and a third-order polynomial fit was used to calculate the mercury concentration. During kinetic measurements an absorption path length between 1 and 100 cm was used, depending on the mercury concentration, to maintain an absorption in the range of our calibration curve.

The molecular chlorine concentration was also determined by in situ UV photometry at 365 nm using a 1 m cell. The literature cross-section of molecular chlorine[18] at 365 nm, 1.06×10^{-19} cm^2, was used.

The initial chlorine atom concentration produced by photolysis was determined from[19]

$$[\mathrm{Cl}] = [\mathrm{Cl_2}] \times \mathrm{QY} \times (1 - \exp[-(P_L/h)(c/\lambda)(\sigma_{\mathrm{Cl_2}}/A_L)]) \quad \text{(I)}$$

where QY is the quantum yield of reaction 3, P_L is the laser power in joules, h is Planck's constant, c is the speed of light in cm s^{-1}, $\sigma_{\mathrm{Cl_2}}$ is the absorbance cross-section at 355 nm in cm^2, λ is the laser wavelength in cm, and A_L is the area of the laser in cm^2. The laser diameter was determined by passing a 0.5 mm pinhole ceramic aperture across the width of the photolysis laser. The transmitted photolysis laser power was recorded in 0.05 cm steps. From the observed beam profile the laser diameter in the reaction volume was determined to be 0.8 ± 0.1 cm. The laser power was measured before and after the LIF cell and then averaged for each decay. This was done to account for reflection loss on the windows, the small absorption of the laser before reaching the detection volume, and any variation in the laser power. The averaged laser power was used for the calculation of the chlorine atom production.

Fluorescence was detected by two PMTs positioned perpendicular to the direction of propagation of the laser beams. The PMT signals were typically averaged for 50 laser pulses by a 500 MHz digital scope and logged on a computer. The temporal profiles of the LIF signals were then constructed by varying the delay time between the photolysis and probe lasers using a digital delay generator.

Cl Atom LIF Detection. The Cl atom concentration was monitored by a two-photon LIF excitation scheme described previously in the literature.[20] This excitation scheme involves the two-photon excitation of the spin forbidden 4p $^4S^0_{3/2}$−3p^5 $^2P^0_{3/2}$ transition near 233 nm with subsequent fluorescence detection near 755 nm from the 4p $^4S^0_{3/2}$−4s ^4P_J transition as shown in Figure 3. The 233 nm probe laser, with a typical output power of 400 μJ, was generated by mixing the frequency doubled output from a dye laser (Spectra Physics PDL3) with the 1064 nm fundamental from a Nd:YAG laser. The fluorescence was detected by a PMT with both an interference filter centered at 755 nm and a 700 nm cutoff filter to eliminate laser stray light. A 60 cm focal length lens was used to focus the laser beam into the detection volume, resulting in a detection limit of 4.0×10^9 molecules cm^{-3} for measurements in 200 Torr of nitrogen.

Hg Atom LIF Detection. The Hg concentration was monitored by exciting the 6p $^3P^0_1$−6s^2 $^1S_0$ transition at 253.7 nm. The excitation beam was generated by a frequency doubled dye laser (Dakota Technologies) with a laser output power in the range of 10 μJ. Resonance fluorescence was observed by a PMT with an interference filter centered at 254 nm. A lens was used to adjust the diameter of the probe beam to about 0.3 cm, less than half the size of the photolysis laser. This size was found to give best results for the detection of mercury while minimizing diffusion related problems. For the mercury LIF the detection limit was less than 9×10^{10} molecules cm^{-3} for low-pressure helium measurements and 2.5×10^{11} molecules cm^{-3} for measurements conducted in air.

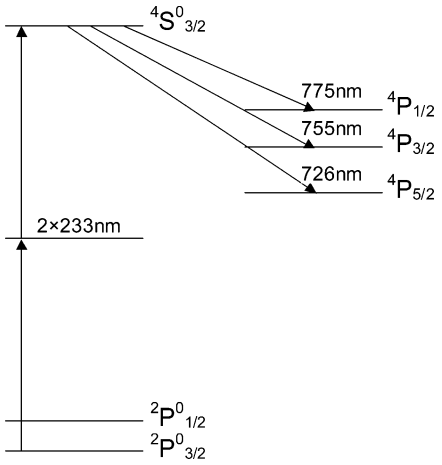

Figure 3. Excitation scheme for the two-photon LIF of Cl atoms. The excitation transition is at 2 × 233 nm with the subsequent fluorescence transition near 755 nm.

Results

Measurements of Hg + Cl + M → HgCl + M (M = He, N_2). Direct determination of rate coefficients for the reactions of gaseous elemental mercury presents a significant experimental challenge due to the low vapor pressure of mercury. This low vapor pressure makes it difficult to study the kinetics of this system using a traditional approach with the stable reactant in pseudo-first-order excess for anything other than reactions with very fast rate coefficients. To overcome this difficulty, we made kinetic measurements under conditions in which chlorine atoms were the reactant in pseudo-first-order excess while simultaneously monitoring the concentration of both reactants.

The rate coefficient for the recombination of mercury and chlorine atoms, reaction 1, was determined with the Cl atom concentrations typically 1000 times larger than the mercury concentration, [Cl] ∼ 1000[Hg]. Both mercury and chlorine atom concentrations were monitored by LIF. The Cl atom concentration was varied between 1.75 and 13×10^{15} molecules cm^{-3}, and Hg concentrations were in the range $(0.4-15) \times 10^{11}$ molecules cm^{-3}.

At the Cl atom concentrations required to observe a significant loss of mercury atoms, the chlorine atom recombination reaction, reaction 2, resulted in a significant decrease in Cl atom concentration on the time scale of the mercury atom decays. Because the Cl atom concentration was not constant, a simple pseudo-first-order decay, i.e., an exponential decay, of the mercury atoms was not observed. Instead, the mercury temporal profiles were fit by numerical integration, and the observed chlorine temporal profiles were analyzed by assuming simple second-order kinetics.

The temporal profiles of the chlorine and mercury atoms were characterized by

$$\frac{d[\mathrm{Hg}]}{dt} = -k_1[\mathrm{Cl}][\mathrm{Hg}][\mathrm{M}] \quad \text{(II)}$$

$$\frac{d[\mathrm{Cl}]}{dt} = -2k_2[\mathrm{Cl}]^2[\mathrm{M}] - k_1[\mathrm{Cl}][\mathrm{Hg}][\mathrm{M}] \quad \text{(III)}$$

Because the concentration of mercury was at least 2 orders of magnitude smaller than the initial Cl atom concentration, the

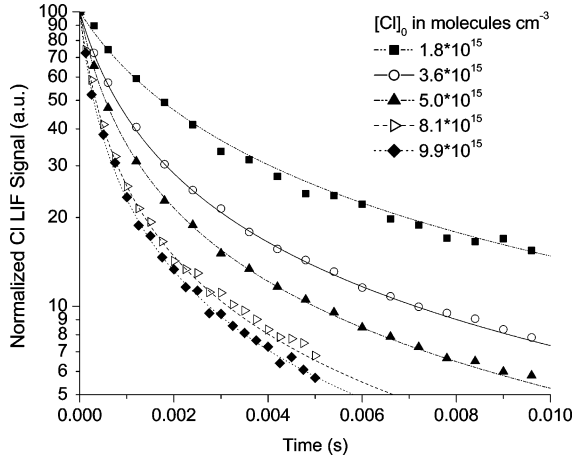

Figure 4. Typical chlorine atom temporal profiles, shown for measurements conducted in 600 Torr N_2 at 293 K.

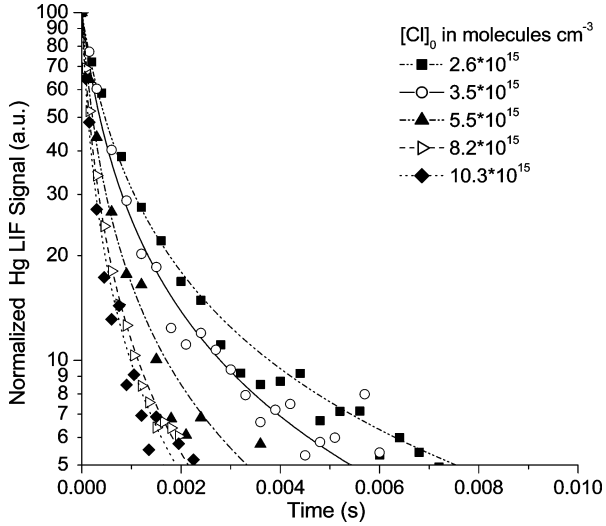

Figure 5. Typical mercury atom temporal profiles, shown for measurements conducted in 600 Torr N_2 at 263 K.

second term in eq III two is negligible and results in a simplified equation

$$\frac{d[Cl]}{dt} = -2k_2[Cl]^2[M] \qquad (IV)$$

For each experimental condition, temporal profiles of chlorine and mercury atoms were measured using LIF. Typical sets of temporal profiles of each atom are shown in Figures 4 and 5. Under each set of conditions, i.e., a fixed pressure, temperature, and initial chlorine atom concentration, the effective second-order rate coefficient, k_2', for the recombination of chlorine atoms was calculated from eq V,

$$\frac{1}{[Cl]_t} = 2k_2't + \frac{1}{[Cl]_0} \qquad (V)$$

which assumes that first-order losses by diffusion and reaction with impurities are negligible. Substituting for [Cl] into eq II gives

$$\frac{d[Hg]}{dt} = -k_1'[Hg]\left(\frac{1}{2k_2't + (1/[Cl]_0)}\right) \qquad (VI)$$

This equation was numerically integrated to give the best fit to the measured mercury profiles and hence a value for k_1', the

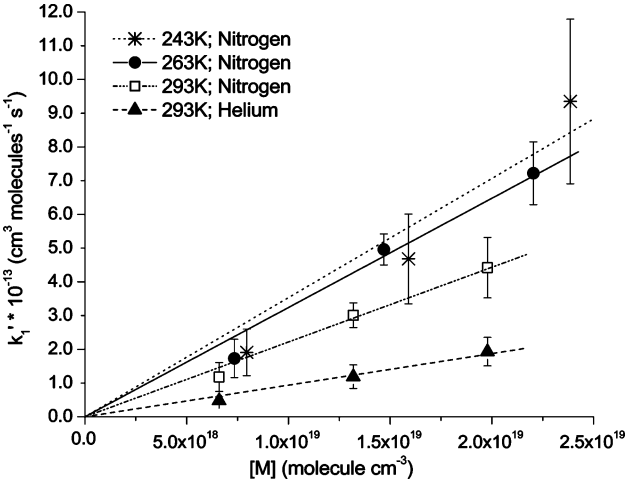

Figure 6. Variation of the effective second-order rate coefficients for the recombination Hg and Cl atoms, k_1', with pressure.

TABLE 1: Second-Order Rate Coefficients for the Recombination of Mercury and Chlorine Atoms, k_1

gas	T (K)	P (Torr)	$10^{13}k_1' \pm 2\sigma$ (cm^3 molecule^{-3} s^{-1})
N_2	243	200	1.91 ± 0.69
		400	4.68 ± 1.33
		600	9.35 ± 2.44
	263	200	1.73 ± 0.57
		400	4.96 ± 0.46
		600	7.18 ± 0.93
	293	200	1.18 ± 0.43
		400	3.01 ± 0.36
		600	4.42 ± 0.90
He	293	200	0.48 ± 0.12
		400	1.19 ± 0.35
		600	1.93 ± 0.42

effective second-order rate coefficient for the recombination of Hg with Cl. The numerical integration procedure was checked by simulating the measured decays using the derived values of k_1' and k_2' in the ACUCHEM program.[21]

The numerically integrated fits to the observed mercury temporal profiles are shown as lines in Figure 5, and the second-order rate coefficients, k_1', obtained in He and N_2 are listed in Table 1. Molecular nitrogen quenched the mercury fluorescence signal efficiently; therefore, the fluorescence yield and thus the S/N ratio degraded with increasing pressure. This was most noticeable in the 243 K data set; however, the overall accuracy of the pressure dependent rate data should not have been significantly affected by this reduction of the S/N ratio.

The third-order recombination rate coefficients were then determined from linear fits of the plots of the second-order rate coefficients, k_1', versus the concentration of N_2 or He, as shown in Figure 6. The plots show the expected linear dependence of rate coefficient versus concentration, indicating that the reaction was in the low-pressure, third-order regime, as might be expected for an atom−atom recombination. However, the plots show a slight negative offset, the magnitude of which increases with temperature. Assuming that the recombination rate coefficients are in the low-pressure limit, the effective second-order rate coefficient should be zero at zero pressure. Consequently, the third-order recombination rate coefficients, k_1, have been calculated by forcing the plots through the origin. The difference between the forced and unforced slopes varied between 10% for the N_2 data at 293 K to 25% for the N_2 data at 243 K. As we show below, similar behavior was observed in the Cl atom recombination data. The third-order recombination rate coef-

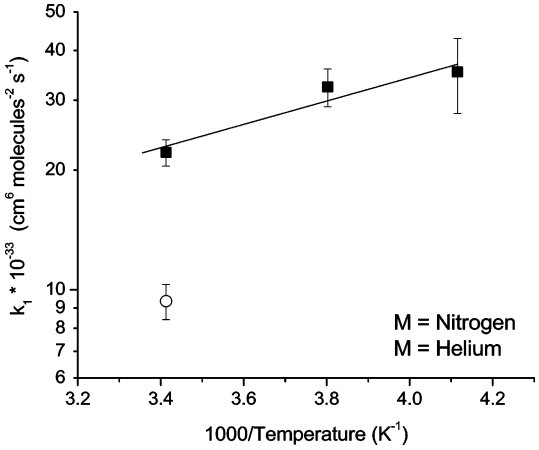

Figure 7. Arrhenius plot of the third-order rate coefficients for the recombination of Hg and Cl atoms, k_1, in N_2 and He.

TABLE 2: Third-Order Rate Coefficients for the Recombination of Mercury and Chlorine Atoms, k_1, Determined in This Work at 293 K in He and 243, 263, and 293 K in N_2, with the Resulting Arrhenius Expression for N_2

gas	T (K)	$10^{33}k_1 \pm 2\sigma$ (cm^6 molecule^{-2} s^{-1})
He	293	9.37 ± 0.95
N_2	243	35.3 ± 7.6
	263	32.4 ± 3.5
	293	22.2 ± 1.7
Arrhenius expression		$(2.2 \pm 0.5) \times 10^{-32} \exp[(680 \pm 400)(1/T - 1/298)]$

ficients, k_1, are listed in Table 2 and plotted in Arrhenius form in Figure 7. The Arrhenius expression for reaction 1 is given by eq VII reported with 2σ errors of precision only. However,

$$k_{1,N_2}(243 - 298\ \mathrm{K}) = (2.2 \pm 0.5) \times 10^{-32} \exp\left[(680 \pm 400)\left(\frac{1}{T} - \frac{1}{298}\right)\right] \quad \text{(VII)}$$

due to uncertainty in the calculation of absolute Cl atom concentrations, which are discussed below; we conservatively estimate the error in the rate coefficient to be ±50%. The observed behavior is consistent with a three-body recombination, demonstrating a positive pressure dependence, an inverse temperature dependence, and a slower rate coefficient in helium than in nitrogen.

Measurements with Mercury in Excess. To confirm the reported mercury chlorine recombination rate coefficient, k_1, measurements were done with mercury in pseudo-first-order excess over chlorine atoms, [Hg] ~ 60[Cl]. Experiments were conducted at 298 K and 200 Torr. A heated permeation tube generated Hg concentrations close to the vapor pressure of mercury at 298 K. Mercury atom and molecular chlorine concentrations were monitored photometrically. The initial Cl atom concentration was kept below 1.0×10^{12} molecules cm^{-3}. The chlorine atom profiles are shown in Figure 8. Under these conditions chlorine atom temporal profiles should follow the simple first-order exponential behavior given by

$$[\mathrm{Cl}]_t = [\mathrm{Cl}]_0 \exp(-k/t) \quad \text{(VIII)}$$

In the third-order low-pressure limit, k' is equal to $k_1[\mathrm{Hg}][\mathrm{M}] + k_d$, where k_d was the background loss of chlorine atoms by self-reaction, reaction with impurities, and loss due to diffusion.

The average of three experiments with no mercury in the cell gave a background chlorine decay rate, k_d, of 79 ± 14 s^{-1}. Four

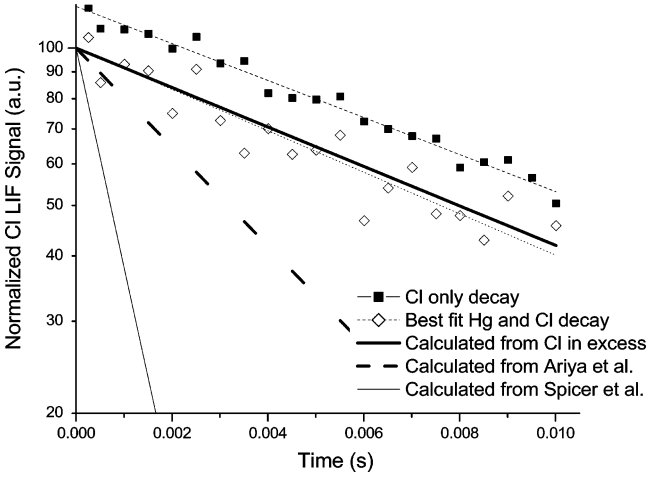

Figure 8. Temporal profile of Cl atoms with mercury in excess concentration. Profiles of Cl in the presence and absence of mercury have been shifted for clarity. The dotted line shows the best fit to the Hg + Cl decay. The thick solid line shows the calculated temporal profile derived from the Arrhenius expression determined from measurements with Cl in excess. Other lines show the calculated temporal profiles based on rate coefficients reported by Ariya et al.[13] and Spicer et al.[14]

measurements were then made with an Hg concentration of 5.3×10^{13} molecules cm^{-3}, for which the decay rate increased to 87 ± 20 s^{-1}. In each case the error represents a 2σ measure of precision only. The difference between the pseudo-first-order decay rates obtained in the two determinations was 8 ± 24 s^{-1}. On the basis of our measured rate coefficient at 293 K and 200 Torr in N_2 and the measured Hg concentration, we would expect an increase in the pseudo-first-order rate of 7.6 s^{-1} (1.43×10^{-13} to 5.3×10^{13}). Hence this measurement, which does not depend on a calculated chlorine atom concentration, is in excellent agreement with the value obtained with chlorine atoms in excess.

Measurements of Cl + Cl + M → Cl_2 + M (M = He, N_2). The determination of temporal profiles of Cl atom concentration was a critical component in measuring the rate coefficient for the mercury and chlorine recombination reaction. The relative concentration profile was determined with good precision using LIF. However, the initial Cl atom concentration was calculated and was, we believe, the largest source of systematic error in the reported rate coefficient for reaction 1. We can, however, make some assessment of the accuracy of this calculation by comparing our measured chlorine atom recombination rate coefficients, which also depends on the accuracy of the Cl atom concentration calibration, with literature values. As shown in Figure 4, chlorine atom temporal profiles were monitored by LIF with the concentration typically followed to 5−20% of the original chlorine atom signal. Under each set of experimental conditions, i.e., a fixed pressure, temperature, and initial chlorine atom concentration, the effective second-order rate coefficient, k_2', for the recombination of Cl atoms was calculated from the Cl temporal profile using eq IX, again assuming a negligible first-order loss due to reaction with impurities or diffusion.

$$\frac{1}{[\mathrm{Cl}]_t} = 2k_2't + \frac{1}{[\mathrm{Cl}]_0} \quad \text{(IX)}$$

Linear fits of plots of 1/[Cl] vs time give the effective second-order recombination rate coefficient, k_2'. Figure 9 shows a series of plots for the reciprocal of absolute chlorine atom concentra-

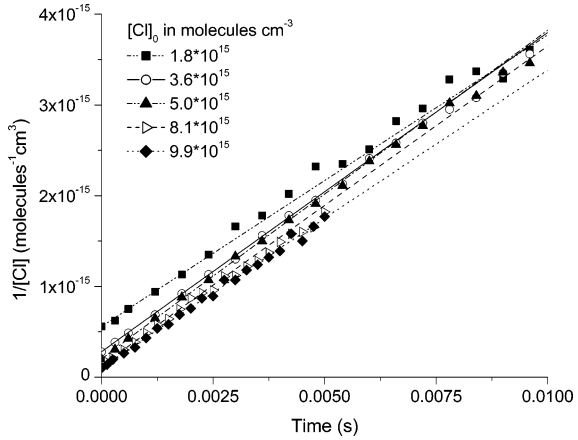

Figure 9. Second-order rate coefficient plot for Cl atom, shown for measurements conducted in 600 Torr N_2 at 293 K.

TABLE 3: Second-Order Rate Coefficients for the Recombination of Chlorine Atoms, k_2

gas	T (K)	P (Torr)	$10^{14}k_2' \pm 2\sigma$ (cm^3 molecule^{-3} s^{-1})
N_2	243	200	9.30 ± 1.97
		400	22.0 ± 5.1
		600	38.7 ± 25.8
	263	200	6.20 ± 1.22
		400	20.9 ± 5.8
		600	30.4 ± 6.9
	293	200	4.41 ± 0.85
		400	11.3 ± 2.0
		600	17.1 ± 1.7
He	293	200	2.65 ± 1.32
		400	6.65 ± 1.20
		600	10.6 ± 1.1

tion versus time. This plot provides an indication of the precision of the data, because all data series under the same temperature and pressure conditions should have the same slope irrespective of initial Cl atom concentration. The data shown in Figure 9 were taken at 293 K in 600 Torr nitrogen buffer gas with initial Cl atom concentrations ranging from 1.8×10^{15} to 9.9×10^{15}. The plots demonstrated excellent linearity and gave an average second-order recombination rate coefficient of $(1.71 \pm 0.17) \times 10^{-13}$ cm^3 molecule^{-1} s^{-1} where the uncertainty is a 2σ error of precision. To ensure that the addition of mercury did not affect the observed Cl atom decay, experiments were conducted in the presence and absence of mercury. The temporal profiles and derived rate coefficients were identical, within the precision of the measurements. This was expected because the Hg concentration was at least 2 orders of magnitude smaller than the initial Cl atom concentration. The values of the effective second-order rate coefficients together with 2σ errors are summarized in Table 3.

The third-order recombination rate coefficients were then determined from linear fits of the plot of second-order rate coefficients, k_2', versus concentration of N_2 or He, as shown in Figure 10. As is the case for the Hg + Cl recombination, the data show a good linear dependence of the effective second-order rate coefficient on pressure. However, we again see a consistent, negative offset. As for reaction 1, the third-order rate coefficients were obtained by forcing all fits through the origin. The forced plots pass through most of the error bars associated with each data point, and the difference in the slopes of the forced and unforced fits varies from 12% to 17%. The third-order recombination rate coefficients, k_2, are listed in Table 4 and plotted in Arrhenius form in Figure 11. For the data in

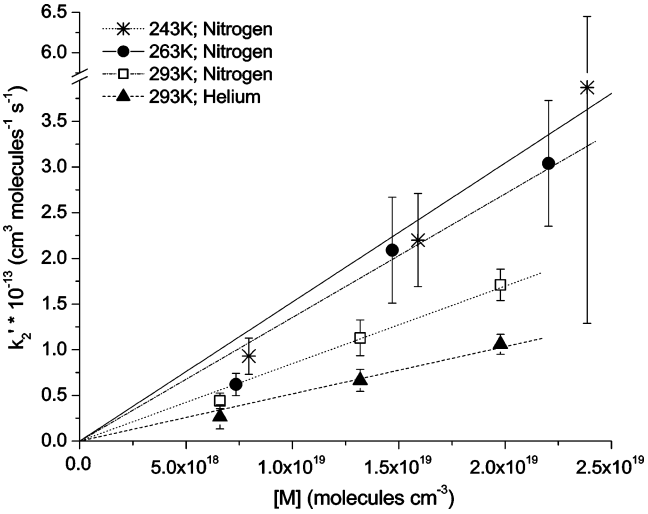

Figure 10. Variation of the effective second-order rate coefficients for the recombination of Cl atoms, k_2', with pressure.

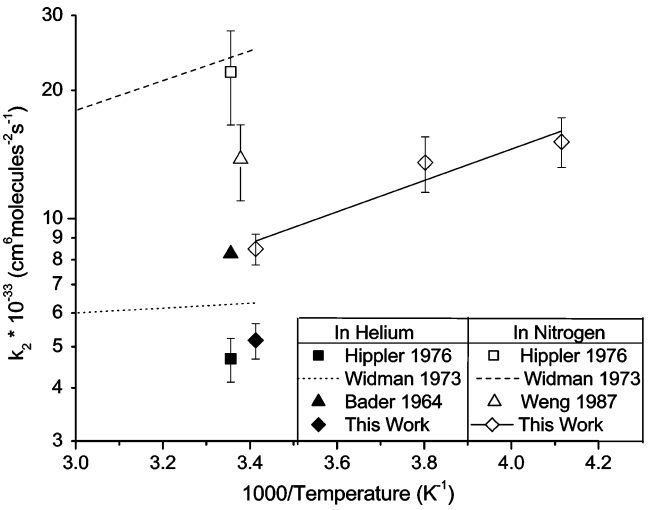

Figure 11. Arrhenius plot of the third-order rate coefficients for the recombination of Cl atoms, k_2, in N_2 and He. Literature values are shown for comparison.

TABLE 4: Third-Order Rate Coefficients for the Recombination of Chlorine Atoms, k_2, Determined in This Work at 293 K in He and 243, 263, and 293 K in N_2, with the Resulting Arrhenius Expression for N_2

gas	T (K)	$10^{33}k_2 \pm 2\sigma$ (cm^6 molecule^{-2} s^{-1})
He	293	5.17 ± 0.49
N_2	243	15.2 ± 2.0
	263	13.5 ± 2.0
	293	8.48 ± 0.71
Arrhenius expression		$(8.4 \pm 2.3) \times 10^{-33} \exp[(850 \pm 470)(1/T - 1/298)]$

nitrogen the resulting Arrhenius expression is given by

$$k_{2,N_2}(243 - 298\ \mathrm{K}) = (8.4 \pm 2.3) \times 10^{-33} \exp\left[(850 \pm 470)\left(\frac{1}{T} - \frac{1}{298}\right)\right] \quad \text{(X)}$$

In eq X the uncertainties are measures of 2σ error of precision only. As we discuss in detail below, we estimate an uncertainty of ±50% in the accuracy of the rate coefficient, due principally to the uncertainty in the calculation of absolute Cl atom concentrations. Overall, the data showed the expected behavior for a three-body recombination, a positive pressure dependence,

an inverse temperature dependence, and a higher deactivation efficiency for nitrogen relative to helium.

Measurements in Air. We observed a large increase in the chlorine atom decay rate in air buffer gas as compared with measurements in N_2. If this loss were solely due to Cl atom recombination, it would have resulted in an increase in the recombination rate coefficient by a factor of 25, implying a 2 orders of magnitude increase in the deactivation efficiency of O_2 relative to N_2. This is not consistent with the expected relative three body efficiencies of nitrogen and oxygen, suggesting an additional loss of Cl atoms due to secondary chemistry.

One possible explanation of the observed increase in the recombination rate coefficient in air is the following reaction sequence (4)−(6):

$$Cl + O_2 + M \leftrightarrow ClO_2 + M \quad (4)$$

$$Cl + ClO_2 \rightarrow Cl_2 + O_2 \quad (5)$$

$$\rightarrow 2ClO \quad (6)$$

To determine if this additional ClO_x chemistry could account for the observed increased loss of Cl atoms, we performed simulations in ACUCHEM[21] using a simplified reaction system consisting of reactions 2 and 4−6. The JPL panel recommended rate coefficients[22] were used for reactions 4−6, and the rate coefficient determined in nitrogen during this work was used for reaction 2. Simulations were also performed using a more complex reaction system, which included the secondary reactions of the products, ClO and ClO_2. However, these reactions were not fast enough to influence the chlorine atom decay and the simplified system was an adequate mechanism. The fits were able to reproduce the increased decay rate within the error range of the rate coefficients and equilibrium constant for reaction 4. Therefore, the proposed ClO_x chemistry can account for the observed increased loss of chlorine atoms.

A significant enhancement in the apparent recombination rate coefficient of mercury and chlorine atoms was also observed in the presence of air. If this loss were solely due to the mercury chlorine recombination reaction, it would have resulted in an increase in the recombination rate coefficient by a factor of 4 relative to the rate coefficient obtained in N_2. Again this is not consistent with the expected relative three-body efficiencies of nitrogen and oxygen and we have chosen not to report a recombination rate coefficient for M═O_2. This observation suggests an additional loss of mercury atoms due to the secondary chemistry described above. Based on this chemistry, the only plausible candidates for reaction with Hg(0) are ClO or ClO_2, and we plan to investigate the reactivity of elemental Hg with these species.

Measurement of the Rate Coefficient for the Reaction Cl + C_2H_6 → Products. Two photon LIF has not been used in this laboratory to monitor Cl atom temporal profiles in kinetics experiments. Therefore, the experimental configuration was tested by measuring the rate coefficient for the reaction of chlorine atoms with ethane.

$$Cl + C_2H_6 \rightarrow C_2H_5 + HCl \quad (7)$$

The rate coefficient, k_7, was determined at 298 K and 200 Torr, using two-photon LIF detection of chlorine atoms with ethane molecules in pseudo-first-order excess concentration, $[C_2H_6] > 500[Cl]$.

Chlorine atom temporal profiles were analyzed assuming simple first-order exponential behavior, where k_7, the rate coefficient for reaction 7, is determined by

$$[Cl]_t = [Cl]_0 \exp(-k_7' t) \quad (XI)$$

where $k_7' = k_7[C_2H_6] + k_d$, and k_d was the background loss of chlorine atoms by diffusion, self-reaction, and reaction with impurities. The pseudo-first-order rate coefficient for reaction 7 was determined at five ethane concentrations ranging from 5×10^{13} to 11×10^{13}. We determined a rate coefficient with a 2σ error of $(5.2 \pm 0.6) \times 10^{-11}$ cm^3 molecule^{-1} s^{-1}, which is in good agreement with the literature value[22] of $(5.7 \pm 1.1) \times 10^{-11}$ cm^3 molecule^{-1} s^{-1}. The good agreement of the rate coefficient determined for reaction 7 by this work and the reference value confirms the viability of the two photon PLP−PLIF system employed in this work to measure Cl atom temporal profiles.

Potential Sources of Systematic Error. As we have noted above, the variation of effective second-order rate coefficients with pressure should show a liner dependence that passes through the origin. In fact, the data consistently show slight negative offsets, which may be indicative of a systematic error in the calculation of the chlorine atom concentration. It should be noted that these offsets were relatively small; in the case of the N_2 data all the intercepts lie within a 4σ error of the origin. The fits also passed within the 2σ errors of precision associated with each data point in most cases.

To calculate the initial chlorine atom concentration, eq I was employed using the absorption cross-section of chlorine molecules at 355 nm, the molecular chlorine concentration, the average laser power, and the laser diameter. The error associated with the first two parameters in eq I should be less than 5%. There was some uncertainty in the laser diameter because the laser beam has a nominally Gaussian intensity profile. As discussed previously, the laser diameter was determined by measuring the laser power through a pinhole across the width of the beam. We estimate the maximum error in the diameter determination to be less than 15%. Finally, we have the error associated with the calibration of the laser power meter, homogeneity within the beam profile, and shot to shot variability, which we estimate gives an uncertainty in the fluence in the range of 25%. We believe that ±50% represents a conservative overall estimate of the uncertainty in the initial Cl atom concentration. As we discuss below, a comparison of our measured Cl atom recombination rates in He, with literature values, suggests that this estimate is reasonable.

Discussion and Comparison with Previous Work

Chlorine Atom Recombination. The chlorine atom recombination reaction rate coefficient, k_2, has been determined in both helium and nitrogen in several studies.[23−27] The results of these studies, including the specific pressure and temperature regimes used are outlined in Table 5 and Figure 11. The agreement between the rate coefficients obtained in this experiment and previous measurements in helium is good. Our reported rates lie between the most recently reported measurements but agree within the respective error limits. The difference between our rate coefficient and the most recent rate coefficient reported by Hippler et al.[25] is less than 10%, and our results are about 20% lower than the value reported by Widman et al. The good agreement between the measurements suggests that our calculation of the initial Cl atom concentration is accurate and the uncertainty estimate is conservative.

The discrepancy between the rate coefficients determined in this work and the previous results in nitrogen is greater. In

TABLE 5: Comparison of Literature Data for Third-Order Rate Coefficients for the Recombination Chlorine Atoms, k_2

gas	T (K)	P (Torr)	k_2 (cm^6 molecule^{-2} s^{-1})	
N_2	296	450−1280	$(1.38 \pm 0.28) \times 10^{-32}$	*a*
	298	760−1520	$(2.21 \pm 0.55) \times 10^{-32}$	*b*
	293−373	760	$1.6 \times 10^{-33} \exp(1.6 \pm 1987/RT)$	*c*
	243−293	200−600	$(8.4 \pm 2.3) \times 10^{-33} \exp[(850 \pm 470)(1/T - 1/298)]$	*e*
He	298	760−1520	$(4.68 \pm 0.55) \times 10^{-33}$	*b*
	298	760	$4.05 \times 10^{-33} \exp(0.26 \pm 9.94(\text{kcal/mol})/RT)$	*c*
	298	1.6−0.4	8.27×10^{-33}	*d*
	293	200−600	$(5.17 \pm 0.49) \times 10^{-33}$	*e*

[a] Reference 27. [b] Reference 25. [c] Reference 26. [d] Referenc 23. [e] This work.

TABLE 6: Reported Rate Coefficients for the Recombination of Mercury and Chlorine Atoms, k_1

gas	T (K)	P (Torr)	k_1		
N_2	298	760	6.4×10^{-11}	cm^3 molecule^{-1} s^{-1}	*a*
	298	760	$(1.0 \pm 0.2) \times 10^{-11}$	cm^3 molecule^{-1} s^{-1}	*b*
	383−443	720	$1.38 \times 10^{-12} \exp(208.02/T)$	cm^3 molecule^{-1} s^{-1}	*c*
	243−293	200−600	$(2.2 \pm 0.5) \times 10^{-32} \exp[(680 \pm 400)(1/T - 1/298)]$	cm^6 molecule^{-2} s^{-1}	*d*
He	243−293	200−600	$(9.37 \pm 0.95) \times 10^{-33}$	cm^6 molecule^{-2} s^{-1}	*d*
CF_3Cl	383−443	720	5.0×10^{-11}	cm^3 molecule^{-1} s^{-1}	*e*
Ar	383−443	720	1.5×10^{-11}	cm^3 molecule^{-1} s^{-1}	*e*

[a] Reference 14. [b] Reference 13. [c] Reference 15. [d] This work. [e] Reference 12.

nitrogen, all data agree within a factor of 3, with the rate coefficient determined in this work being the slowest rate coefficient. The most recently reported data from Weng et al.[27] is 60% faster than our determination; this is within the combined error limits.

We can identify one possible complication in our rate coefficient determination that might account for a systematic discrepancy between the results in He and N_2. A significant impurity in the N_2 might result in additional loss of chlorine atoms by reaction. However, any additional reaction that resulted in the loss of chlorine atoms would increase the observed rate coefficient. Because the rate coefficient that we observed is slower than that in previous studies, it seems unlikely that our system was influenced by this complication. Any other systematic errors should influence the results in He and N_2 in a similar manner.

Mercury and Chlorine Atom Recombination. Three previous experimental determinations[12−14] and one theoretical study[15] have reported values for reaction 1, and these results are compared with the current work in Table 6. Horne et al.[12] used flash photolysis combined with absorption spectroscopy to study reaction 1 at temperatures 383−443 K and 720 Torr. The Horne study reported a rate coefficient for the mercury chlorine recombination of 5.0×10^{-11} cm^3 molecule^{-1} s^{-1} in CF_3Cl and 1.5×10^{-11} cm^3 molecule^{-1} s^{-1} in Ar, with a reported error of a factor of 3.

The rate coefficients obtained are not directly comparable to those reported here, due to temperature and buffer gas differences. However, the large difference in the rate coefficients cannot be reasonably explained by the differences in experimental conditions. Among the potential problems associated with this experiment, two appear to be particularly significant. First, the system was a static system where a gas mixture undergoes repeated flashes. This experimental approach increases the possibility of secondary chemistry, product photolysis, and interfering species. Second, to determine the rate coefficient for reaction 1, it was necessary to determine the absolute mercury chloride (HgCl) concentration. Horne et al. determined mercury chloride concentrations by determining the loss of mercury and assuming that all the mercury that is lost in the system is converted to mercury chloride. This determination could have a large uncertainty and could be influenced by secondary loss processes of mercury. These complications could lead to significant errors in the calculation of the absolute concentration.

Two more recent studies have utilized relative rate techniques at pressures of one atmosphere and at room temperature. Ariya et al.[13] reported a rate coefficient of $(1.0 \pm 0.2) \times 10^{-11}$ cm^3 molecule^{-1} s^{-1}. This study was conducted in a static 2 or 3 L Pyrex flask. Five different reference molecules were used obtaining results, which differed by a factor of 270 in the measured relative rates together with a strong nonlinearity of the relative rate plot when determined in a bath gas of air. They concluded that the variation was caused by the presence of a secondary reaction between the reference molecules and OH. The buffer gas was switched from air to nitrogen to eliminate oxygen chemistry, giving an overall reduction in the observed rate. However, the variation in the measured relative rate between the reference molecules was still a factor of 30 and the nonlinearity remained. Ultimately, a series of 8 measurements were made using 1,3-dichloropropane as the reference molecule, and the addition of 835 ppm of benzene, as an OH scavenger. The reported rate coefficient was determined from this small subset of the data.

The second relative rate study, Spicer et al.,[14] was performed on much more limited set of experiments monitoring mercury loss relative to that of dimethyl sulfide (DMS) in air. This work was performed in a 17.3 m^3 environmental chamber. Ultimately, Spicer et al. reported a value of 6.4×10^{-11} cm^3 molecule^{-1} s^{-1}.

The large dependence of the measured relative rate coefficient on the identity of the reference compound demonstrates clearly that the study of Ariya et al. was influenced by secondary chemistry. The large discrepancy observed between measurement in air and nitrogen, and the nonlinearity observed in the relative rate plots in both bath gases, are further confirmation of this. Ariya et al. attribute the secondary chemistry to the formation of OH but offer no mechanism for OH formation in nitrogen buffer. It should also be noted that an enhanced removal of the reference compound by secondary chemistry would produce an under-estimate of the rate coefficient. However, the rate coefficients obtained in both competitive rate studies exceed any reasonable theoretical estimate of the rate coefficient. We feel that a more plausible explanation would be additional loss

of mercury, either by heterogeneous reaction or possibly by a gas-phase reaction with an oxygenated species, like ClO. An additional process that removed mercury would generate the observed faster rate coefficient.

Figure 8 shows the experimental temporal profiles of chlorine atoms in the presence and absence of mercury at its saturation vapor pressure. As we show above, the difference between the pseudo-first-order decay rate, $8 \pm 24\ s^{-1}$, agrees well with that calculated from our measured rate coefficient with Cl atoms in excess, $7.6\ s^{-1}$. However the calculated pseudo-first-order decay rates using the rate coefficients reported in the competitive rate studies would be much larger. Assuming a linear dependence on pressure, the rate coefficient reported by Ariya et al. would produce an increase in the pseudo-first-order decay rate of 139 s^{-1} (2.63×10^{-12} to 5.3×10^{13}) in the presence of mercury. As shown in Figure 8, this would lead to an overall pseudo-first-order decay rate of 218 s^{-1}, which would be clearly distinguishable from the decay in the absence of mercury. The increase in pseudo-first-order decay rate calculated from the rate coefficient of Spicer et al. would be even larger, 893 s^{-1} (1.68×10^{-11} to 5.3×10^{13}). The temporal profiles calculated using these rate coefficients are shown in Figure 8, and it is clear that they are not compatible with our experimental data.

Khalizov et al.[15] determined the recombination rate coefficient for reaction 1 using electronic structure calculations to obtain both molecular parameters and the capture rate or high-pressure limit. Once this high-pressure limit was obtained, Khalizov et al. determined a pressure dependent rate coefficient by assuming a strong collisional deactivation. To compare this with the observed data, it is essential to consider the mechanism of a three-body recombination. A three-body recombination consists of an initial collision that generates an excited complex, reaction 8. A portion of the excited complex will directly decompose back into reactants, reaction 9, whereas the other portion undergoes an collision and is stabilized, reaction 10.

$$Hg + Cl \rightarrow HgCl^* \quad (8)$$

$$HgCl^* \rightarrow Hg + Cl \quad (9)$$

$$HgCl^* + M \rightarrow HgCl + M \quad (10)$$

The calculated pressure dependent rate coefficient reported by Khalizov et al. assumed that every collision of the buffer gas with the initially formed energized HgCl* complex deactivated the complex to produce a stable HgCl molecule that cannot dissociate to products. This typically unrealistic assumption should produce the maximum possible recombination rate coefficient at any particular pressure. The value they obtained, 2.8×10^{-12} cm^3 molecule^{-1} s^{-1} at 298 K, 760 Torr, is a factor of 3 smaller than the rate coefficient reported by Ariya et al. and a factor of 20 smaller than that reported by Spicer et al. On the other hand, this rate coefficient is a factor of 5 faster that the rate coefficient report in this work. This difference can be attributed to the fact that not all collisions with the buffer gas will transfer sufficient energy to stabilize the molecule, resulting in a slower rate coefficient.

In this work the measurement of k_1, was performed under two experimental configurations at room temperature. First, the rate coefficients were obtained with chlorine in excess, where an absolute determination of the chlorine atom concentration was necessary. For confirmation, a limited set of experiments were performed in a second configuration with mercury in excess, where it was not necessary to determine the absolute chlorine atom concentration. There is good agreement between these two rate coefficient determinations. This agreement suggests that the determination of the initial chlorine atom concentration is not a source of significant error for either reaction 1 or reaction 2. We would also note that this is the first study of reaction 1 that has systematically varied the temperature, pressure, and buffer gases. The observed behavior was entirely consistent with the behavior expected for a three-body recombination.

Conclusions

We have reported recombination rate coefficients for the reaction of mercury and chlorine atoms, k_1, together with the self-reaction of chlorine atoms, k_2. In both cases the rate coefficients show pressure, temperature, and third-body deactivation efficiencies that are consistent with three-body recombination. For reaction 1, the recombination of chlorine with mercury, we obtain rate coefficients that are much smaller than previously reported results. For this reaction measurements were conducted in two experimental configurations with either mercury or chlorine atoms in excess; both methods obtained similar results. The large discrepancy observed between this work and the previous studies questions the viability of using the relative rate method to determine kinetic rate coefficients for mercury halogen reactions. For reaction 2, the self-reaction of chlorine atoms, we obtain results that are in good agreement with literature values in helium buffer gas. The rate coefficient obtained in nitrogen is smaller than those obtained in prior studies.

To evaluate the importance of the recombination of elemental mercury and chlorine atoms, an effective second-order rate coefficient of 7.6×10^{-13} cm^3 molecule^{-1} s^{-1} was calculated from the reported Arrehenius expression for Arctic conditions, 260 K and 760 Torr. Assuming a peak concentration[28] of chlorine atoms of 10^4-10^5 cm^{-3}, the lifetime of mercury due to reaction with chlorine atoms is between 4.2 years and 152 days. This suggests that the recombination reaction of mercury with chlorine atoms does not contribute significantly to the chemistry of mercury depletion events.

Acknowledgment. This research has been supported by a grant from the U.S. Environmental Protection Agency's Science to Achieve Results (STAR) program.

References and Notes

(1) Facemire, C.; Augspurger, T.; Bateman, D.; Brim, M.; Conzelmann, P.; Delchamps, S.; Douglas, E.; Inmon, L.; Looney, K.; Lopez, F.; Masson, G.; Morrison, D.; Morse, N.; Robison, A. *Water Air Soil Pollution* **1995**, *80*, 923.

(2) Meyer, M. W.; Evers, D. C.; Daulton, T.; Braselton, W. E. *Water Air Soil Pollution* **1995**, *80*, 871.

(3) Keating, M.; Mahaffey, K.; Schoeny, R.; Rice, G.; Bullock, O. R.; Ambrose, R.; Swantout, J.; Nichols, J. Mercury Study Report to Congress. United States Environmental Protection Agency Office of Air Quality Planning & Standards and Office of Research and Development, 1997.

(4) Lin, C. J.; Pehkonen, S. O. *Atmos. Environ.* **1999**, *33*, 2067.

(5) Schroeder, W. H.; Anlauf, K. G.; Barrie, L. A.; Lu, J. Y.; Steffen, A.; Schneeberger, D. R.; Berg, T. *Nature* **1998**, *394*, 331.

(6) Lindberg, S. E.; Brooks, S.; Lin, C. J.; Scott, K. J.; Landis, M. S.; Stevens, R. K.; Goodsite, M.; Richter, A. *Environ. Sci. Technol.* **2002**, *36*, 1245.

(7) Ebinghaus, R.; Kock, H. H.; Temme, C.; Einax, J. W.; Lowe, A. G.; Richter, A.; Burrows, J. P.; Schroeder, W. H. *Environ. Sci. Technol.* **2002**, *36*, 1238.

(8) Temme, C.; Einax, J. W.; Ebinghaus, R.; Schroeder, W. H. *Environ. Sci. Technol.* **2003**, *37*, 22.

(9) Skov, H.; Christensen, J. H.; Goodsite, M. E.; Heidam, N. Z.; Jensen, B.; Wahlin, P.; Geernaert, G. *Environ. Sci. Technol.* **2004**, *38*, 2373.

(10) Berg, T.; Bartnicki, J.; Munthe, J.; Lattila, H.; Hrehoruk, J.; Mazur, A. *Atmos. Environ.* **2001**, *35*, 2569.

(11) Vogt, R.; Crutzen, P. J.; Sander, R. *Nature* **1996**, *383*, 327.

(12) Horne, D. G.; Gosavi, R.; Strausz, O. P. *J. Chem. Phys.* **1968**, *48*, 4758.
(13) Ariya, P. A.; Khalizov, A.; Gidas, A. *J. Phys. Chem. A* **2002**, *106*, 7310.
(14) Spicer, C. W.; Satola, J.; Abbgy, A. A.; Plastridge, R. A.; Cowen, K. A. Kinetics of Gas-Phase Elemental Mercury Reaction with Halogen Species, Ozone, and Nitrate Radical under Atmospheric Conditions. Florida Department of Environmental Protection, 2002.
(15) Khalizov, A. F.; Viswanathan, B.; Larregaray, P.; Ariya, P. A. *J. Phys. Chem. A* **2003**, *107*, 6360.
(16) Busch, G. E.; Mahoney, R. T.; Morse, R. I. *J. Chem. Phys.* **1969**, *51*, 449.
(17) Burkholder, J. B.; Bair, E. J. *J. Phys. Chem.* **1983**, *87*, 1859.
(18) Maric, D.; Burrows, J. P.; Meller, R.; Moortgat, G. K. *Journal of Photochem. Photobiol. A-Chem.* **1993**, *70*, 205.
(19) Rodgers, M. O.; Asai, K.; Davis, D. D. *Appl. Opt.* **1980**, *19*, 3597.
(20) Sappey, A. D.; Jeffries, J. B. *Appl. Phys. Lett.* **1989**, *55*, 1182.
(21) Braun, W.; Herron, J. T.; Kahaner, D. ACUCHEM/ACUPLOT; National Bureau of Standards: Gaithersburg, MD, 1986.
(22) Sander, S. P.; Finlayson-Pitts, B. J.; Friedl, R. R.; Golden, D. M.; Huie, R. E.; Kolb, C. E.; Kurylo, M. J.; Molina, M. J.; Moortgat, G. K.; Orkin, V. L.; Ravishankara, A. R. Chemical Kinetics and Photochemical Data for Use in Atmosperic Studies, Evaluation Number 14. JPL publication 02-25; Jet Propulsion Laboratory: Pasadena, CA, 2002.
(23) Bader, L. W.; Ogryzlo, E. A. *Nature* **1964**, *201*, 491.
(24) Hippler, H.; Troe, J. *Chem. Phys. Lett.* **1973**, *19*, 607.
(25) Hippler, H.; Troe, J. *Int. J. Chem. Kinet.* **1976**, *8*, 501.
(26) Widman, R. P.; DeGraff, B. A. *J. Phys. Chem.* **1973**, *77*, 1325.
(27) Weng, C. J.; Ho, T. I.; Su, T. M. *J. Phys. Chem.* **1987**, *91*, 5235.
(28) Boudries, H.; Bottenheim, J. W. *Geophys. Res. Lett.* **2000**, *27*, 517.